FERMILAB-PUB-12-017-E

Search for a low mass Standard Model Higgs boson in the $\tau\tau$ decay channel in $p\bar{p}$ collisions at $\sqrt{s} = 1.96$ TeV

T. Aaltonen,[21] B. Álvarez González[w],[9] S. Amerio,[41] D. Amidei,[32] A. Anastassov,[36] A. Annovi,[17] J. Antos,[12] G. Apollinari,[15] J.A. Appel,[15] A. Apresyan,[46] T. Arisawa,[56] A. Artikov,[13] J. Asaadi,[51] W. Ashmanskas,[15] B. Auerbach,[59] A. Aurisano,[51] F. Azfar,[40] W. Badgett,[15] A. Barbaro-Galtieri,[26] V.E. Barnes,[46] B.A. Barnett,[23] P. Barria[dd],[44] P. Bartos,[12] M. Bauce[bb],[41] G. Bauer,[30] F. Bedeschi,[44] D. Beecher,[28] S. Behari,[23] G. Bellettini[cc],[44] J. Bellinger,[58] D. Benjamin,[14] A. Beretvas,[15] A. Bhatti,[48] M. Binkley*,[15] D. Bisello[bb],[41] I. Bizjak[ii],[28] K.R. Bland,[5] B. Blumenfeld,[23] A. Bocci,[14] A. Bodek,[47] D. Bortoletto,[46] J. Boudreau,[45] A. Boveia,[11] B. Brau[a],[15] L. Brigliadori[aa],[6] A. Brisuda,[12] C. Bromberg,[33] E. Brucken,[21] M. Bucciantonio[cc],[44] J. Budagov,[13] H.S. Budd,[47] S. Budd,[22] K. Burkett,[15] G. Busetto[bb],[41] P. Bussey,[19] A. Buzatu,[31] C. Calancha,[29] S. Camarda,[4] M. Campanelli,[33] M. Campbell,[32] F. Canelli[11],[15] A. Canepa[ii],[60] B. Carls,[22] D. Carlsmith,[58] R. Carosi,[44] S. Carrillo[k],[16] S. Carron,[15] B. Casal,[9] M. Casarsa,[15] A. Castro[aa],[6] P. Catastini,[20] D. Cauz,[52] V. Cavaliere,[22] M. Cavalli-Sforza,[4] A. Cerri[f],[26] L. Cerrito[q],[28] Y.C. Chen,[1] M. Chertok,[7] G. Chiarelli,[44] G. Chlachidze,[15] F. Chlebana,[15] K. Cho,[25] D. Chokheli,[13] J.P. Chou,[20] W.H. Chung,[58] Y.S. Chung,[47] C.I. Ciobanu,[42] M.A. Ciocci[dd],[44] A. Clark,[18] C. Clarke,[57] G. Compostella[bb],[41] M.E. Convery,[15] J. Conway,[7] M.Corbo,[42] M. Cordelli,[17] C.A. Cox,[7] D.J. Cox,[7] F. Crescioli[cc],[44] C. Cuenca Almenar,[59] J. Cuevas[w],[9] R. Culbertson,[15] D. Dagenhart,[15] N. d'Ascenzo[u],[42] M. Datta,[15] P. de Barbaro,[47] S. De Cecco,[49] G. De Lorenzo,[4] M. Dell'Orso[cc],[44] C. Deluca,[4] L. Demortier,[48] J. Deng[c],[14] M. Deninno,[6] F. Devoto,[21] M. d'Errico[bb],[41] A. Di Canto[cc],[44] B. Di Ruzza,[44] J.R. Dittmann,[5] M. D'Onofrio,[27] S. Donati[cc],[44] P. Dong,[15] M. Dorigo,[52] T. Dorigo,[41] K. Ebina,[56] A. Elagin,[51] A. Eppig,[32] R. Erbacher,[7] D. Errede,[22] S. Errede,[22] N. Ershaidat[z],[42] R. Eusebi,[51] H.C. Fang,[26] S. Farrington,[40] M. Feindt,[24] J.P. Fernandez,[29] C. Ferrazza[ee],[44] R. Field,[16] G. Flanagan[s],[46] R. Forrest,[7] M.J. Frank,[5] M. Franklin,[20] J.C. Freeman,[15] Y. Funakoshi,[56] I. Furic,[16] M. Gallinaro,[48] J. Galyardt,[10] J.E. Garcia,[18] A.F. Garfinkel,[46] P. Garosi[dd],[44] H. Gerberich,[22] E. Gerchtein,[15] S. Giagu[ff],[49] V. Giakoumopoulou,[3] P. Giannetti,[44] K. Gibson,[45] C.M. Ginsburg,[15] N. Giokaris,[3] P. Giromini,[17] M. Giunta,[44] G. Giurgiu,[23] V. Glagolev,[13] D. Glenzinski,[15] M. Gold,[35] D. Goldin,[51] N. Goldschmidt,[16] A. Golossanov,[15] G. Gomez,[9] G. Gomez-Ceballos,[30] M. Goncharov,[30] O. González,[29] I. Gorelov,[35] A.T. Goshaw,[14] K. Goulianos,[48] S. Grinstein,[4] C. Grosso-Pilcher,[11] R.C. Group[55],[15] J. Guimaraes da Costa,[20] Z. Gunay-Unalan,[33] C. Haber,[26] S.R. Hahn,[15] E. Halkiadakis,[50] A. Hamaguchi,[39] J.Y. Han,[47] F. Happacher,[17] K. Hara,[53] D. Hare,[50] M. Hare,[54] R.F. Harr,[57] K. Hatakeyama,[5] C. Hays,[40] M. Heck,[24] J. Heinrich,[43] M. Herndon,[58] S. Hewamanage,[5] D. Hidas,[50] A. Hocker,[15] W. Hopkins[g],[15] D. Horn,[24] S. Hou,[1] R.E. Hughes,[37] M. Hurwitz,[11] U. Husemann,[59] N. Hussain,[31] M. Hussein,[33] J. Huston,[33] G. Introzzi,[44] M. Iori[ff],[49] A. Ivanov[o],[7] E. James,[15] D. Jang,[10] B. Jayatilaka,[14] E.J. Jeon,[25] M.K. Jha,[6] S. Jindariani,[15] W. Johnson,[7] M. Jones,[46] K.K. Joo,[25] S.Y. Jun,[10] T.R. Junk,[15] T. Kamon,[51] P.E. Karchin,[57] A. Kasmi,[5] Y. Kato[n],[39] W. Ketchum,[11] J. Keung,[43] V. Khotilovich,[51] B. Kilminster,[15] D.H. Kim,[25] H.S. Kim,[25] H.W. Kim,[25] J.E. Kim,[25] M.J. Kim,[17] S.B. Kim,[25] S.H. Kim,[53] Y.K. Kim,[11] N. Kimura,[56] M. Kirby,[15] S. Klimenko,[16] K. Kondo,[56] D.J. Kong,[25] J. Konigsberg,[16] A.V. Kotwal,[14] M. Kreps,[24] J. Kroll,[43] D. Krop,[11] N. Krumnack[l],[5] M. Kruse,[14] V. Krutelyov[d],[51] T. Kuhr,[24] M. Kurata,[53] S. Kwang,[11] A.T. Laasanen,[46] S. Lami,[44] S. Lammel,[15] M. Lancaster,[28] R.L. Lander,[7] K. Lannon[v],[37] A. Lath,[50] G. Latino[cc],[44] T. LeCompte,[2] E. Lee,[51] H.S. Lee,[11] J.S. Lee,[25] S.W. Lee[x],[51] S. Leo[cc],[44] S. Leone,[44] J.D. Lewis,[15] A. Limosani[r],[14] C.-J. Lin,[26] J. Linacre,[40] M. Lindgren,[15] E. Lipeles,[43] A. Lister,[18] D.O. Litvintsev,[15] C. Liu,[45] Q. Liu,[46] T. Liu,[15] S. Lockwitz,[59] A. Loginov,[59] D. Lucchesi[bb],[41] J. Lueck,[24] P. Lujan,[26] P. Lukens,[15] G. Lungu,[48] J. Lys,[26] R. Lysak,[12] R. Madrak,[15] K. Maeshima,[15] K. Makhoul,[30] S. Malik,[48] G. Manca[b],[27] A. Manousakis-Katsikakis,[3] F. Margaroli,[46] C. Marino,[24] M. Martínez,[4] R. Martínez-Ballarín,[29] P. Mastrandrea,[49] M.E. Mattson,[57] P. Mazzanti,[6] K.S. McFarland,[47] P. McIntyre,[51] R. McNulty[i],[27] A. Mehta,[27] P. Mehtala,[21] A. Menzione,[44] C. Mesropian,[48] T. Miao,[15] D. Mietlicki,[32] A. Mitra,[1] H. Miyake,[53] S. Moed,[20] N. Moggi,[6] M.N. Mondragon[k],[15] C.S. Moon,[25] R. Moore,[15] M.J. Morello,[15] J. Morlock,[24] P. Movilla Fernandez,[15] A. Mukherjee,[15] Th. Muller,[24] P. Murat,[15] M. Mussini[aa],[6] J. Nachtman[m],[15] Y. Nagai,[53] J. Naganoma,[56] I. Nakano,[38] A. Napier,[54] J. Nett,[51] C. Neu,[55] M.S. Neubauer,[22] J. Nielsen[e],[26] L. Nodulman,[2] O. Norniella,[22] E. Nurse,[28] L. Oakes,[40] S.H. Oh,[14] Y.D. Oh,[25] I. Oksuzian,[55] T. Okusawa,[39] R. Orava,[21] L. Ortolan,[4] S. Pagan Griso[bb],[41] C. Pagliarone,[52] E. Palencia[f],[9] V. Papadimitriou,[15] A.A. Paramonov,[2] J. Patrick,[15] G. Pauletta[gg],[52] M. Paulini,[10] C. Paus,[30] D.E. Pellett,[7] A. Penzo,[52] T.J. Phillips,[14] G. Piacentino,[44] E. Pianori,[43] J. Pilot,[37] K. Pitts,[22] C. Plager,[8] L. Pondrom,[58] K. Potamianos,[46] O. Poukhov*,[13] F. Prokoshin[y],[13]

Operated by Fermi Research Alliance, LLC under Contract No. De-AC02-07CH11359 with the United States Department of Energy.

A. Pronko,[15] F. Ptohos[h],[17] E. Pueschel,[10] G. Punzi[cc],[44] J. Pursley,[58] A. Rahaman,[45] V. Ramakrishnan,[58] N. Ranjan,[46] I. Redondo,[29] P. Renton,[40] M. Rescigno,[49] T. Riddick,[28] F. Rimondi[aa],[6] L. Ristori[45],[15] A. Robson,[19] T. Rodrigo,[9] T. Rodriguez,[43] E. Rogers,[22] S. Rolli,[54] R. Roser,[15] M. Rossi,[52] F. Rubbo,[15] F. Ruffini[dd],[44] A. Ruiz,[9] J. Russ,[10] V. Rusu,[15] A. Safonov,[51] W.K. Sakumoto,[47] Y. Sakurai,[56] L. Santi[gg],[52] L. Sartori,[44] K. Sato,[53] V. Saveliev[u],[42] A. Savoy-Navarro,[42] P. Schlabach,[15] A. Schmidt,[24] E.E. Schmidt,[15] M.P. Schmidt[*],[59] M. Schmitt,[36] T. Schwarz,[7] L. Scodellaro,[9] A. Scribano[dd],[44] F. Scuri,[44] A. Sedov,[46] S. Seidel,[35] Y. Seiya,[39] A. Semenov,[13] F. Sforza[cc],[44] A. Sfyrla,[22] S.Z. Shalhout,[7] T. Shears,[27] P.F. Shepard,[45] M. Shimojima[t],[53] S. Shiraishi,[11] M. Shochet,[11] I. Shreyber,[34] A. Simonenko,[13] P. Sinervo,[31] A. Sissakian[*],[13] K. Sliwa,[54] J.R. Smith,[7] F.D. Snider,[15] A. Soha,[15] S. Somalwar,[50] V. Sorin,[4] P. Squillacioti,[15] M. Stancari,[15] M. Stanitzki,[59] R. St. Denis,[19] B. Stelzer,[31] O. Stelzer-Chilton,[31] D. Stentz,[36] J. Strologas,[35] G.L. Strycker,[32] Y. Sudo,[53] A. Sukhanov,[16] I. Suslov,[13] K. Takemasa,[53] Y. Takeuchi,[53] J. Tang,[11] M. Tecchio,[32] P.K. Teng,[1] J. Thom[g],[15] J. Thome,[10] G.A. Thompson,[22] E. Thomson,[43] P. Ttito-Guzmán,[29] S. Tkaczyk,[15] D. Toback,[51] S. Tokar,[12] K. Tollefson,[33] T. Tomura,[53] D. Tonelli,[15] S. Torre,[17] D. Torretta,[15] P. Totaro,[41] M. Trovato[ee],[44] Y. Tu,[43] F. Ukegawa,[53] S. Uozumi,[25] A. Varganov,[32] F. Vázquez[k],[16] G. Velev,[15] C. Vellidis,[3] M. Vidal,[29] I. Vila,[9] R. Vilar,[9] J. Vizán,[9] M. Vogel,[35] G. Volpi[cc],[44] P. Wagner,[43] R.L. Wagner,[15] T. Wakisaka,[39] R. Wallny,[8] S.M. Wang,[1] A. Warburton,[31] D. Waters,[28] M. Weinberger,[51] W.C. Wester III,[15] B. Whitehouse,[54] D. Whiteson[c],[43] A.B. Wicklund,[2] E. Wicklund,[15] S. Wilbur,[11] F. Wick,[24] H.H. Williams,[43] J.S. Wilson,[37] P. Wilson,[15] B.L. Winer,[37] P. Wittich[g],[15] S. Wolbers,[15] H. Wolfe,[37] T. Wright,[32] X. Wu,[18] Z. Wu,[5] K. Yamamoto,[39] J. Yamaoka,[14] T. Yang,[15] U.K. Yang[p],[11] Y.C. Yang,[25] W.-M. Yao,[26] G.P. Yeh,[15] K. Yi[m],[15] J. Yoh,[15] K. Yorita,[56] T. Yoshida[j],[39] G.B. Yu,[14] I. Yu,[25] S.S. Yu,[15] J.C. Yun,[15] A. Zanetti,[52] Y. Zeng,[14] and S. Zucchelli[aa6]

(CDF Collaboration[†])

[1]*Institute of Physics, Academia Sinica, Taipei, Taiwan 11529, Republic of China*
[2]*Argonne National Laboratory, Argonne, Illinois 60439, USA*
[3]*University of Athens, 157 71 Athens, Greece*
[4]*Institut de Fisica d'Altes Energies, ICREA, Universitat Autonoma de Barcelona, E-08193, Bellaterra (Barcelona), Spain*
[5]*Baylor University, Waco, Texas 76798, USA*
[6]*Istituto Nazionale di Fisica Nucleare Bologna, [aa]University of Bologna, I-40127 Bologna, Italy*
[7]*University of California, Davis, Davis, California 95616, USA*
[8]*University of California, Los Angeles, Los Angeles, California 90024, USA*
[9]*Instituto de Fisica de Cantabria, CSIC-University of Cantabria, 39005 Santander, Spain*
[10]*Carnegie Mellon University, Pittsburgh, Pennsylvania 15213, USA*
[11]*Enrico Fermi Institute, University of Chicago, Chicago, Illinois 60637, USA*
[12]*Comenius University, 842 48 Bratislava, Slovakia; Institute of Experimental Physics, 040 01 Kosice, Slovakia*
[13]*Joint Institute for Nuclear Research, RU-141980 Dubna, Russia*
[14]*Duke University, Durham, North Carolina 27708, USA*
[15]*Fermi National Accelerator Laboratory, Batavia, Illinois 60510, USA*
[16]*University of Florida, Gainesville, Florida 32611, USA*
[17]*Laboratori Nazionali di Frascati, Istituto Nazionale di Fisica Nucleare, I-00044 Frascati, Italy*
[18]*University of Geneva, CH-1211 Geneva 4, Switzerland*
[19]*Glasgow University, Glasgow G12 8QQ, United Kingdom*
[20]*Harvard University, Cambridge, Massachusetts 02138, USA*
[21]*Division of High Energy Physics, Department of Physics, University of Helsinki and Helsinki Institute of Physics, FIN-00014, Helsinki, Finland*
[22]*University of Illinois, Urbana, Illinois 61801, USA*
[23]*The Johns Hopkins University, Baltimore, Maryland 21218, USA*
[24]*Institut für Experimentelle Kernphysik, Karlsruhe Institute of Technology, D-76131 Karlsruhe, Germany*
[25]*Center for High Energy Physics: Kyungpook National University, Daegu 702-701, Korea; Seoul National University, Seoul 151-742, Korea; Sungkyunkwan University, Suwon 440-746, Korea; Korea Institute of Science and Technology Information, Daejeon 305-806, Korea; Chonnam National University, Gwangju 500-757, Korea; Chonbuk National University, Jeonju 561-756, Korea*
[26]*Ernest Orlando Lawrence Berkeley National Laboratory, Berkeley, California 94720, USA*
[27]*University of Liverpool, Liverpool L69 7ZE, United Kingdom*
[28]*University College London, London WC1E 6BT, United Kingdom*
[29]*Centro de Investigaciones Energeticas Medioambientales y Tecnologicas, E-28040 Madrid, Spain*
[30]*Massachusetts Institute of Technology, Cambridge, Massachusetts 02139, USA*

[31]*Institute of Particle Physics: McGill University, Montréal, Québec, Canada H3A 2T8; Simon Fraser University, Burnaby, British Columbia, Canada V5A 1S6; University of Toronto, Toronto, Ontario, Canada M5S 1A7; and TRIUMF, Vancouver, British Columbia, Canada V6T 2A3*
[32]*University of Michigan, Ann Arbor, Michigan 48109, USA*
[33]*Michigan State University, East Lansing, Michigan 48824, USA*
[34]*Institution for Theoretical and Experimental Physics, ITEP, Moscow 117259, Russia*
[35]*University of New Mexico, Albuquerque, New Mexico 87131, USA*
[36]*Northwestern University, Evanston, Illinois 60208, USA*
[37]*The Ohio State University, Columbus, Ohio 43210, USA*
[38]*Okayama University, Okayama 700-8530, Japan*
[39]*Osaka City University, Osaka 588, Japan*
[40]*University of Oxford, Oxford OX1 3RH, United Kingdom*
[41]*Istituto Nazionale di Fisica Nucleare, Sezione di Padova-Trento, [bb]University of Padova, I-35131 Padova, Italy*
[42]*LPNHE, Universite Pierre et Marie Curie/IN2P3-CNRS, UMR7585, Paris, F-75252 France*
[43]*University of Pennsylvania, Philadelphia, Pennsylvania 19104, USA*
[44]*Istituto Nazionale di Fisica Nucleare Pisa, [cc]University of Pisa, [dd]University of Siena and [ee]Scuola Normale Superiore, I-56127 Pisa, Italy*
[45]*University of Pittsburgh, Pittsburgh, Pennsylvania 15260, USA*
[46]*Purdue University, West Lafayette, Indiana 47907, USA*
[47]*University of Rochester, Rochester, New York 14627, USA*
[48]*The Rockefeller University, New York, New York 10065, USA*
[49]*Istituto Nazionale di Fisica Nucleare, Sezione di Roma 1, [ff]Sapienza Università di Roma, I-00185 Roma, Italy*
[50]*Rutgers University, Piscataway, New Jersey 08855, USA*
[51]*Texas A&M University, College Station, Texas 77843, USA*
[52]*Istituto Nazionale di Fisica Nucleare Trieste/Udine, I-34100 Trieste, [gg]University of Udine, I-33100 Udine, Italy*
[53]*University of Tsukuba, Tsukuba, Ibaraki 305, Japan*
[54]*Tufts University, Medford, Massachusetts 02155, USA*
[55]*University of Virginia, Charlottesville, Virginia 22906, USA*
[56]*Waseda University, Tokyo 169, Japan*
[57]*Wayne State University, Detroit, Michigan 48201, USA*
[58]*University of Wisconsin, Madison, Wisconsin 53706, USA*
[59]*Yale University, New Haven, Connecticut 06520, USA*
[60]*TRIUMF, Vancouver, British Columbia, Canada V6T 2A3*
(Dated: January 23, 2012)

We report on a search for the standard model Higgs boson decaying into pairs of τ leptons in $p\bar{p}$ collisions produced by the Tevatron at $\sqrt{s} = 1.96$ TeV. The analyzed data sample was recorded by the CDFII detector and corresponds to an integrated luminosity of 6.0 fb^{-1}. The search is performed in the final state with one τ decaying leptonically and the second one identified through its semi-hadronic decay. Since no significant excess is observed, a 95% credibility level upper limit on the production cross section times branching ratio to the $\tau\tau$ final state is set for hypothetical Higgs boson masses between 100 and 150 GeV/c^2. For a Higgs boson of 120 GeV/c^2 the observed (expected) limit is 14.6 (15.3) the predicted value.

PACS numbers: 14.80.Bn, 14.60.Fg, 13.85.Rm

*Deceased
†With visitors from [a]University of MA Amherst, Amherst, MA 01003, USA, [b]Istituto Nazionale di Fisica Nucleare, Sezione di Cagliari, 09042 Monserrato (Cagliari), Italy, [c]University of CA Irvine, Irvine, CA 92697, USA, [d]University of CA Santa Barbara, Santa Barbara, CA 93106, USA, [e]University of CA Santa Cruz, Santa Cruz, CA 95064, USA, [f]CERN,CH-1211 Geneva, Switzerland, [g]Cornell University, Ithaca, NY 14853, USA, [h]University of Cyprus, Nicosia CY-1678, Cyprus, [i]University College Dublin, Dublin 4, Ireland, [j]University of Fukui, Fukui City, Fukui Prefecture, Japan 910-0017, [k]Universidad Iberoamericana, Mexico D.F., Mexico, [l]Iowa State University, Ames, IA 50011, USA, [m]University of Iowa, Iowa City, IA 52242, USA, [n]Kinki University, Higashi-Osaka City, Japan 577-8502, [o]Kansas State University, Manhattan, KS 66506, USA, [p]University of Manchester, Manchester M13 9PL, United Kingdom, [q]Queen Mary, University of London, London, E1 4NS, United Kingdom, [r]University of Melbourne, Victoria 3010, Australia, [s]Muons, Inc., Batavia, IL 60510, USA, [t]Nagasaki Institute of Applied Science, Nagasaki, Japan, [u]National Research Nuclear University, Moscow, Russia, [v]University of Notre Dame, Notre Dame, IN 46556, USA, [w]Universidad de Oviedo, E-33007 Oviedo, Spain, [x]Texas Tech University, Lubbock, TX 79609, USA, [y]Universidad Tecnica Federico Santa Maria, 110v Valparaiso,

Spontaneous electroweak symmetry breaking (EWSB) has been introduced in the standard model (SM) to explain how fundamental particles acquire mass. In the SM, EWSB requires the existence of a yet unobserved scalar particle, the Higgs boson [1–3]. Direct searches at LEP [4], combined with the recent exclusion mass ranges provided by the Tevatron [5] and LHC experiments [6], have reduced the possible values for the mass of the SM Higgs boson. The Higgs mass is now excluded at 95% confidence level (C.L.) below 114 GeV/c^2 and between 141 and 476 GeV/c^2. A global fit to electroweak measurements [7] provides indirect indications that confirm the region below 158 GeV/c^2 as the most probable. Therefore the searches in the low mass decay channels play a crucial role to set a final statement on the SM Higgs boson existence.

Although the Higgs boson decay into a pair of τ leptons is not the dominant process in the low mass regime, searches in this final state are important for several reasons. First, the inclusion of additional channels improves overall sensitivity of the search. Also, once the Higgs boson is discovered, measurements of its decay branching ratios (B.R.'s) into different channels can give important information about its true nature. Furthermore, when beyond SM scenarios are considered, such the minimal supersymmetric extension of the SM (MSSM) [8], the study of final states containing τ leptons attracts even more interest, given their enhanced coupling to the Higgs bosons in large regions of the model parameter space.

A previous search for the SM Higgs boson in the final states with τ leptons was performed by the D0 Collaboration [9]. This Letter presents results of a search for the $H \to \tau\tau$ decays in the final state with two τ leptons and one or more jets, using a data sample corresponding to an integrated luminosity of 6.0 fb^{-1} of $p\bar{p}$ collisions collected at the Tevatron by the CDFII detector at $\sqrt{s}$ = 1.96 TeV. The search is sensitive to contributions of several Higgs boson production mechanisms: gluon-gluon fusion $gg \to H$, associated production with the W or Z boson (VH), and the vector boson fusion (VBF) $qHq' \to q\tau\tau q'$. To improve the search sensitivity a novel strategy for the τ identification is proposed, based on a multivariate technique [10]. Tau leptons are short-lived particles (τ = 290.6 × 10^{-15} s [11]), which can be detected only through their decay products. Semi-hadronic decays $\tau \to X_h \nu_\tau$, where X_h is a system of hadrons and ν_τ is the τ neutrino, are denoted in this paper as τ_h and correspond to a B.R. of about 65%. With leptonic decays $\tau_l \to l\nu_l\nu_\tau$ accounting for the remaining 35%, the final states $\tau_h\tau_l$, studied in this paper include about 46% of all possible decays of τ pairs.

CDFII [12–14] is an azimuthally and forward-backward symmetric general-purpose particle detector. The geometry is described using the azimuthal angle φ and the pseudo-rapidity $\eta = -\ln\tan(\theta/2)$, where θ is the polar angle measured with respect to the proton beam axis z. A charged-particle tracking system, immersed in a 1.4 T solenoidal magnetic field, consists of an inner set of silicon micro-strip detectors ($|\eta| < 2$), and a open-cell drift chamber ($|\eta| < 1$). Electromagnetic and hadronic sampling calorimeters surround the tracking system and cover central ($|\eta| < 1.1$) and forward ($1.1 < |\eta| < 3.6$) regions. Proportional chambers and scintillating strip detectors, embedded in the electromagnetic section of the central and forward calorimeters correspondingly, measure positions and transverse profiles of the showers. Dedicated muon detectors located outside the calorimeter provide coverage for $|\eta| < 1.5$. Gas Cherenkov counters, installed in the forward region $3.7 < |\eta| < 4.7$, measure the average number of inelastic interactions per bunch crossing, providing a measurement of the instantaneous luminosity. The components of energy and momenta in the plane transverse to the beam are defined as $E_T = E\sin\theta$ and $p_T = p\sin\theta$. Since neutrinos do not interact with the detector components, their E_T must be inferred from the energy imbalance in the transverse plane, $\not\!\!E_T$ [15].

Data for this search have been collected using a trigger selection [14] which requires one central electron or muon candidate with $\mathrm{p}_T > 8$ GeV/c and one additional isolated track with $\mathrm{p}_T > 5$ GeV/c [16], which is used as a starting point for the τ_h reconstruction.

Jets are reconstructed from clustered energy depositions in the calorimeter towers using a fixed cone algorithm [17] with a radius in the φ-η space $\Delta R = \sqrt{\Delta\varphi^2 + \Delta\eta^2} < 0.4$. Jets are required to have $|\eta| < 2.5$, an electromagnetic fraction $E_{em}/E < 0.9$, and $E_T > 20$ GeV, where the transverse energy is corrected for instrumental effects and multiple $p\bar{p}$ collisions in the event [17].

At the analysis level, an electron candidate is reconstructed as a calorimeter cluster with $\mathrm{E}_T > 10$ GeV pointed to by a well-measured track. The candidate is required to have a shower mostly contained in the electromagnetic compartment, and the lateral shape of the shower must be consistent with test beam measurements. A muon candidate is reconstructed from a track with $p_T >$ 10 GeV/c, matching to the track segments in the muon chambers. Muon energy deposition in the calorimeter should be consistent with that of a minimum-ionizing particle. Electron and muon reconstruction is described in detail in Ref. [14].

In the detector, semi-hadronic decays of the τ leptons manifest themselves as narrow jets with low track multiplicity. A τ_h candidate is required to have a good quality track with $\mathrm{p}_T > 6$ GeV/c, pointing to a calorimeter cluster with $E_T > 9$ GeV and $|\eta| < 1.0$. Momenta of the charged and neutral particles reconstructed around the

---

Chile, [z]Yarmouk University, Irbid 211-63, Jordan, [hh]University of Pennsylvania, Philadelphia, Pennsylvania 19104, USA, [ii]On leave from J. Stefan Institute, Ljubljana, Slovenia,

highest p_T track in the cluster (referred to as the seed track [18]), define the "visible" four-momentum of the τ_h candidate, $\vec{p}_{vis}$. The transverse component of $\vec{p}_{vis}$, or visible p_T, is required to be greater than 15 GeV/c. Momenta of the neutral pions and photons are reconstructed using the central shower maximum detector. To be consistent with the topology of the hadronic τ decay, the number of tracks associated with the τ_h candidate is required to be 1 or 3. Tau decay modes with higher charged track multiplicity, contributing of the order of 1%, are not considered. Contamination from electrons and muons mimicking the τ_h signature is reduced by rejecting candidates with $E_{had}/P < 0.2$, where E_{had} is the hadronic part of the τ_h cluster energy, and P is the scalar sum of all track momenta associated with the τ_h candidate. To discriminate between taus and jets originating from quarks or gluons (referred to as QCD jets), the reconstructed τ_h candidates are required to be isolated. This is achieved by demanding that no charged or neutral particles are reconstructed in the isolation annulus [18] defined around the seed track, or by requiring the sum of their measured p_T to be below a given threshold. In this search, the discrimination between τ_h's and QCD jets is further enhanced by using a multivariate selection based on a set of Boosted Decision Trees (BDTs) [19, 20]. Several τ_h categories are defined according to the number of tracks and to the visible p_T of the τ_h candidate, and specific BDTs are implemented for each category. The input variables which provide the largest discrimination power are the τ_h visible mass, $M_{vis} = \sqrt{p^2_{\rm vis}}$, and the number of charged and neutral particles reconstructed in the isolation annulus, as well as the sum of their p_T. Compared to the cut-based τ_h selection [21], the BDT-based selection reduces the jet $\to \tau_h$ misidentification rate by 25% while maintaining the same identification efficiency, at a level of 35% for $p_T > 30$ GeV/c.

The two identified τ leptons in the event must have opposite charges and be spatially separated, $\Delta R > 0.4$. In addition, selected events are required to have a good quality vertex with $|V_z| < 60$ cm, where V_z is the vertex z-coordinate.

The irreducible background contributions to this search originate from Z+jets, $t\bar{t}$ and diboson events with one τ_h and an electron (or muon) in the final state. Another source of background events is due to lepton misidentification in γ+jet, QCD multijet and W+jets production. $Z \to ee/\mu\mu$ events can satisfy the selection criteria when one of the two electrons or muons is mistakenly identified as a τ_h candidate. This contribution is suppressed by vetoing events containing a τ_h with $E_{had}/P < 0.4$ and the dilepton invariant mass $M_{l\tau}$ consistent with that of the Z boson.

The signal and background estimates are based on a combination of Monte Carlo (MC) simulations and data-driven methods. The detector response is simulated with a GEANT3-based package [22]. Higgs, $t\bar{t}$

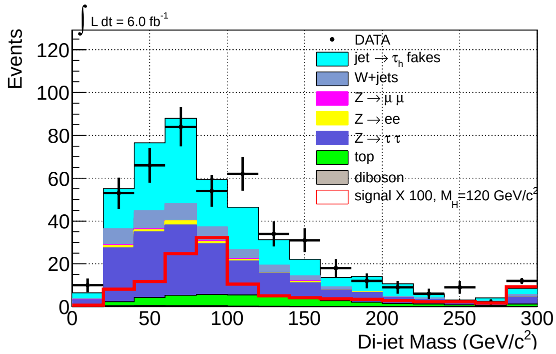

FIG. 1: Invariant mass of the two most energetic jets, in the N(jets) ≥ 2 channel.

and diboson production processes are generated by PYTHIA [23] with the CTEQ5L set of parton distribution functions (PDF's) [24] and their contributions normalized to the next-to-leading order (NLO) theoretical cross sections [25–29]. The Z+jets background is generated using ALPGEN [30], matched with PYTHIA for the hadronization and parton showering. Relative contributions of the different Z+n partons subprocesses are provided by ALPGEN, with the total event yield normalized to the measured $Z \to ll$ production cross section [31]. Additional correction factors, determined by comparing data and simulations in specific control samples, are applied to account for the observed mis-modeling of the $e/\mu \to \tau_h$ misidentification probabilities. Background contributions resulting from lepton misidentification are estimated using a data-based method. In γ+jet and QCD multijet events no significant correlation is expected between the charges of the two reconstructed lepton candidates, thus leading to an equal amount of opposite-sign (OS) and same-sign (SS) events with similar kinematic features. The γ+jet and QCD multijet contributions in the OS event selection are then modeled using the SS data sample. In case of the W+jets process there is a correlation between the charge of the lepton produced in the W boson decay and the charge of the outgoing quark which generates the jet misidentified as the τ_h; this results in an excess of OS events. This OS/SS asymmetry, A = 2.2 ± 0.5, is measured in a W+jets enriched control sample obtained by loosening the τ_h selection and by applying a cut on $\not{E}_T > 20/30/35$ GeV (for events with N(jets) = 0, 1 or ≥ 2, respectively) and on the reconstructed W transverse mass, $M_T > 40$ GeV/c [32].

We split the analysis sample into three subsamples according to the number of reconstructed jets in the final state. Events with N(jets) = 0 are used to validate the background model. The τ_h identification efficiency, ϵ, is measured in a high purity $Z \to \tau\tau$ sample, defined by events with N(jets) = 0, $\not{E}_T > 10$ GeV and $M_T < 60$ GeV/c^2. The ratio of the ϵ measurements in the data and MC, $SF_\tau = 0.96 \pm 0.05$, is used to correct the ac-

TABLE I: Expected event yields in the two signal channels, compared to the number of observed events. Quoted errors include both systematic and statistical uncertainties.

Process	N(jets) = 1	N(jets) ≥ 2
$Z \to \tau\tau$	935 ± 85	160 ± 24
$Z \to$ ee	30.6 ± 3.9	6.8 ± 1.0
$Z \to \mu\mu$	15.5 ± 2.7	1.9 ± 0.5
$WW/WZ/ZZ$	9.3 ± 1.0	2.2 ± 0.3
$t\bar{t}$	11.3 ± 1.6	39.3 ± 4.6
jet→ τ fakes	1219 ± 124	171 ± 19
W+jets	151 ± 38	46.8 ± 14.1
Total background	2371 ± 156	428 ± 36
$gg \to H$	1.42 ± 0.45	0.34 ± 0.24
WH	0.23 ± 0.03	0.39 ± 0.05
ZH	0.13 ± 0.02	0.25 ± 0.03
VBF	0.18 ± 0.02	0.25 ± 0.03
Total signal (M_H = 120 GeV/c^2)	1.96 ± 0.45	1.23 ± 0.29
Data	2517	462

ceptance. Expected signal and background yields and the observed data in the N(jets) = 1 and N(jets) ≥ 2 channels are summarized in Table I. Figure 1 shows the invariant mass of the two most energetic jets in the N(jets) ≥ 2 channel; since the hadronic decay of the W or Z boson is reconstructed, this variable is one of the most powerful in discriminating the associated Higgs boson production signal from the largest backgrounds.

Several sources of systematic uncertainties affect both the signal and background estimates. The largest one is the uncertainty on the jet energy scale [17], which leads to acceptance variations up to a 20% level in different jet multiplicity channels. Non-negligible effects on the shapes of different jet-related kinematic distributions are also observed and taken into account. Another relevant source of systematic uncertainty which affects the sample normalizations is the theoretical and experimental uncertainty on the cross sections: uncertainties on diboson and $t\bar{t}$ production are 6% and 10% respectively [25–27], while for Drell-Yan processes we take a value of 2.2% [31]. The $gg \to H$ production depends strongly on the gluon parton density function and the accompanying value of α_s(q^2). The theoretical uncertainty on the cross section of this process, calculated separately for different jet multiplicity channels, results in uncertainties of 23.5% and 67.5% on the expected yield of the signal events with N(jets) = 1 and N(jets) ≥ 2, respectively [28]. The cross section uncertainties for the other Higgs boson production mechanisms are 10% for VBF and 5% for VH [25, 29]. The uncertainties on the τ_h identification efficiency and on the e $\to \tau_h$ and $\mu \to \tau_h$ misidentification probabilities, are 5%, 7%, and 15% respectively. Systematic uncertainties due to the modeling of the initial state (ISR) and final state radiation (FSR) have been evaluated for all the Higgs boson production processes: the largest variation, 15%, corresponds to the gluon fusion process. The choice of the PDFs affects the acceptance at the level of a few percent, while an uncertainty of 2.3% on the inclusive Drell-Yan acceptance is derived from the differences between the observed ALPGEN and PYTHIA-based calculations. A 10% uncertainty on the contribution of events with jets misidentified as τ_h is estimated from SS data. The uncertainty of the W+jets background is estimated, using OS/SS asymmetry, at 25% (30%) for W + 1 (≥ 2) jet channel.

After all selection cuts are applied, the background expectation is still significantly larger than the expected Higgs boson signal. The dominant irreducible background contribution, Z→ $\tau\tau$, is topologically very similar to the signal, thus affecting the sensitivity of the search; in addition, the Higgs boson invariant mass reconstructed from the visible decay products of the two τ leptons suffers from a very poor resolution, given that a sizeable fraction of the τ energy is carried by the undetected neutrinos. Since no other single powerful variable is available, a multivariate approach is followed and the discriminating power of various kinematic and topological observables is combined into one single output discriminant. The search strategy is based on two sequential BDT-based selections applied to the candidate events. The first set of BDTs is trained to discriminate $H \to \tau\tau$ from W+jets, QCD, $Z \to ee/\mu\mu$ and $t\bar{t}$ backgrounds. At this step an event is accepted if its BDT score is higher than an optimal value, estimated by maximizing the search sensitivity. The second set of BDTs is trained to discriminate the signal against $Z \to \tau\tau$. The choice and the number of input variables is optimized for each BDT, considering the most discriminating among a set of 23 well-modeled kinematic quantities. The training procedure is performed separately for the N(jets) = 1 and N(jets) ≥ 2 channels and optimized for two different Higgs boson mass scenarios (M_H = 120 GeV/c^2 and M_H = 140 GeV/c^2). Results are shown in Fig. 2 for a Higgs boson mass of 120 GeV/c^2.

The observed number of events in the two channels, as well as the distributions in the BDT output variables, are consistent with the SM background expectations, so we use the BDT output templates to set 95% C.L. upper limits on the SM Higgs boson production. A Bayesian likelihood method [11] with a flat prior assigned to the signal cross section is employed, and all statistical and systematic shape and rate uncertainties are appropriately incorporated. The two channels are combined, and the resulting limits are shown in Fig. 3 and summarized in Table II. For all mass values, the expected and observed limits are within one standard deviation from each other.

We presented in this Letter the results of the search for the Higgs boson in the $\tau\tau$ decay mode, using final states involving one hadronically decaying τ lepton. This measurement contributes to the sensitivity of the low mass Higgs boson searches at the Tevatron. The value of the expected (observed) limit for a Higgs boson mass of 120

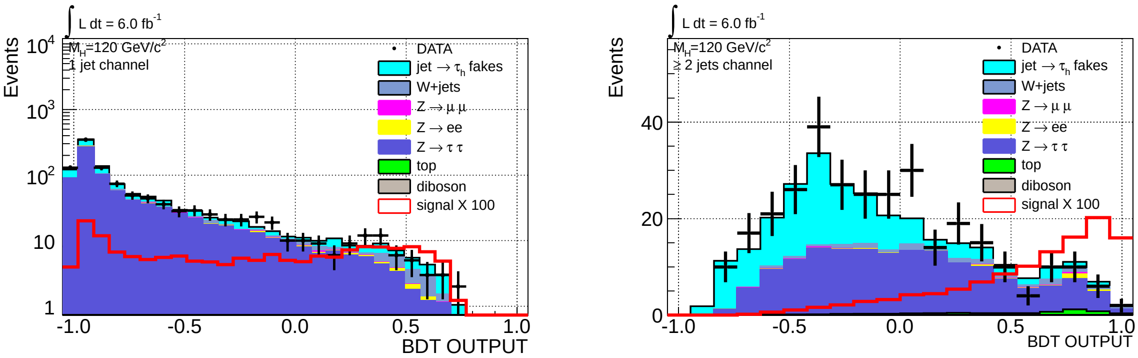

FIG. 2: Final discriminant distributions for the $N(\text{jets}) = 1$ and $N(\text{jets}) \geq 2$ jets channels, obtained by combining a set of BDTs trained to discriminate a 120 GeV/c^2 Higgs boson signal from the main sources of background.

TABLE II: Expected and observed 95% C.L. upper limits on $\sigma(p\bar{p} \to H)B.R.(H \to \tau\tau)$, relative to the theoretical SM prediction.

M_H (GeV/c^2)	100	105	110	115	120	125	130	135	140	145	150
Expected	18.9	17.5	15.7	15.2	15.3	16.9	19.4	23.6	29.7	40.9	62.0
Observed	19.6	18.1	15.5	14.7	14.6	16.4	18.7	22.6	33.7	47.3	70.2

GeV/c^2 is 15.3 (14.6) times the SM expectation.

We thank the Fermilab staff and the technical staffs of the participating institutions for their vital contributions. This work was supported by the U.S. Department of Energy and National Science Foundation; the Italian Istituto Nazionale di Fisica Nucleare; the Ministry of Education, Culture, Sports, Science and Technology of Japan; the Natural Sciences and Engineering Research Council of Canada; the National Science Council of the Republic of China; the Swiss National Science Foundation; the A.P. Sloan Foundation; the Bundesministerium für Bildung und Forschung, Germany; the Korean World Class University Program, the National Research Foundation of Korea; the Science and Technology Facilities Council and the Royal Society, UK; the Institut National de Physique Nucleaire et Physique des Particules/CNRS; the Russian Foundation for Basic Research; the Ministerio de Ciencia e Innovación, and Programa Consolider-Ingenio 2010, Spain; the Slovak R&D Agency; the Academy of Finland; and the Australian Research Council (ARC).

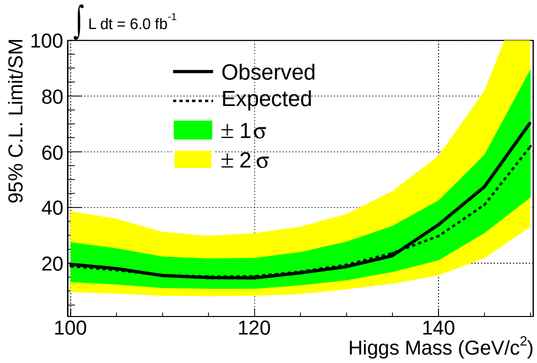

FIG. 3: Expected (dashed curve) and observed (solid curve) 95% C.L. upper limit on $\sigma(p\bar{p} \to H)B(H \to \tau\tau)$, as a function of the mass, in the range between 100 and 150 GeV/c^2.

[1] P. Higgs, Phys. Rev. Lett. **13**, 508 (1964).
[2] F. Englert and R. Brout, Phys. Rev. Lett. **13**, 321 (1964).
[3] G. Guralnik*et al.*, Phys. Rev. Lett. **13**, 585 (1964).
[4] G. Abbiendi, Phys. Lett. B **565**, 61 (2003).
[5] CDF and D0 Coll., The Tevatron New Phenomena, Higgs Working Group, arXiv:1107.5518[hep-ex] (2011).
[6] ATLAS and CMS Coll., ATLAS-CONF-2011-157,CMS PAS HIG-11-023 (2011).
[7] ALEPH Collaboration *et al.*, arxiv:1012.2367[hep-ex] (2010).
[8] D.J.H. Chung *et al.*, Phys. Rept. **407** (2005)
[9] V.M. Abazov *et al.* (D0 Collaboration), Phys. Rev. Lett. **102**, 251801 (2009).
[10] P. Totaro, Ph.D. Thesis, University of Trieste, FERMILAB-THESIS-2011-38(2011)
[11] K. Nakamura *et al.* (Particle Data Group), J. Phys. G **37**, 075021 (2010).
[12] D. Acosta *et al.* (CDF Collaboration), Phys. Rev. D **71**, 032001 (2005).
[13] D. Acosta *et al.* (CDF Collaboration), Phys. Rev. D **71**, 052003 (2005).
[14] A. Abulencia *et al.* (CDF Collaboration), J. Phys. G Nucl. Part. Phys. **34**, 2457 (2007).
[15] The missing E_T ($\not\!\!E_T$) is defined as the magnitude of the vector $\vec{\not\!\!E}_T = -\sum_i E_T^i \hat{n}_i$, where i is the calorimeter tower number with $|\eta| < 3.6$, while $\hat{n}_i$ is a unit vector perpendicular to the beam axis and pointing at the center of the ith calorimeter tower.
[16] At trigger level, a track is isolated if no additional tracks

with $p_T > 1.5$ GeV/c are reconstructed within 10 and 30 degrees around the track direction.
[17] A. Bhatti *et al.*, Nucl. Instrum. Methods A**566**, 375 (2006).
[18] The τ_h reconstruction is based on a two-cone algorithm: the 3D angles $\theta_{sig} = \min(0.17, 5.0\ \text{GeV}/E_{clu})$ and $\theta_{iso} = 0.52$ rad, where E_{clu} is the cluster energy, define a signal cone and a isolation annulus around the highest p_T track.
[19] A. Hoecker *et al.*, Proc. Sci **ACAT2007**, 040 (2007).
[20] L. Breiman *et al.*, *Classification and Regression Trees*, Wadsworth and Brooks, Monterey, CA (1984).
[21] A. Abulencia *et al.*, Phys. Rev. D **75**, 092004 (2007).
[22] R. Brun *et al.*, CERN-DD-78-2-REV, CERN-DD-78-2.
[23] T. Sjostrand *et al.*, J. High Energy Phys. **0605** 026 (2006).
[24] H.L. Lai *et al.* (CTEQ Collaboration), Eur. Phys. J. C **12**, 375-392 (2000).
[25] J.M. Campbell and R.K. Ellis, http://mcfm.fnal.gov.
[26] J.M. Campbell and R.K. Ellis, Phys. Rev. D **60**, 113006 (1999).
[27] U. Langenfeld, S. Moch, and P. Uwer, Phys. Rev. D **80**, 054009 (2009).
[28] C. Anastasiou, R. Boughezal, and F. Petriello, J. High Energy Phys. **0908** 099 (2009).
[29] J. Baglio and A. Djouadi, J. High Energy Phys. **1010** 064 (2010).
[30] M.L. Mangano *et al.*, J. High Energy Phys. **0307** 001 (2003).
[31] D. Acosta *et al.*, Phys. Rev.Lett. **94**, 091803 (2005).
[32] $\mathrm{M}_T = \sqrt{2 p_T \not\!\!E_T (1 - \cos\theta_{l\nu})}$, where p_T is the transverse momentum of the identified electron (or muon) in the final state and $\theta_{l\nu}$ is the azimuthal angle between the lepton and the direction of $\not\!\!E_T$.